Journal of Health, Wellness and Community Research
ISSN: 3007, 0570

OPEN ACCESS

JHWCR

Type: Original Article
Published: 29 September 2025
Volume: III, **Issue:** XIII
DOI: https://doi.org/10.61919/4nzm4d83

Correspondence
✉ Nida Ambreen, nidaambreen@awkum.edu.pk

Received 16, 08, 25
Accepted 25, 09, 2025

Authors' Contributions
Concept: NA AA; Design: NA ZP; Data Collection: SK MA SF BK RN; Analysis: AA ZP NA; Drafting: AA NA

Declarations
No funding was received for this study. The authors declare no conflict of interest. The study received ethical approval. All participants provided informed consent.

"Click to Cite"

Exploring *Paeonia emodi's*, Phytochemical Potential: Extraction, Quantification and Bioassays Studies

Arshid Ali[1], Nida Ambreen[2], Zahida Parveen[1], Saira Farman[1], Beenish Khurshid[1], Sania Badar[3], Mehreen Ilyas[3], Sohrab Khan[2], Reema Naz[2]

1 Department of Biochemistry, Abdul Wali Khan University Mardan, Mardan, Pakistan
2 Department of Chemistry, Abdul Wali Khan University Mardan, Mardan, Pakistan
3 Department of Biological Sciences, Superior University, Lahore, Pakistan

ABSTRACT

Background: *Type 2 diabetes features postprandial hyperglycaemia, impaired insulin signalling, and glyco-oxidative stress. Approaches that simultaneously attenuate intestinal carbohydrate digestion, enhance insulin receptor signalling, and limit advanced glycation end-products (AGEs) may offer superior benefit.* ***Objective:*** *To quantify phytochemical constituents of Paeonia emodi roots and assess multitarget antidiabetic activities—antiglycation, α-amylase and α-glucosidase inhibition, and PTP1B inhibition—across phytochemical classes and solvent fractions.* ***Methods:*** *Roots were ethanolic-extracted and successively fractionated with n-hexane, chloroform, ethyl acetate, and methanol. Total flavonoids, phenolics, and tannins were measured by $AlCl_3$ and Folin methods; alkaloids were determined gravimetrically. Bioactivities were evaluated in microplates: BSA–glucose antiglycation (Ex/Em 370/440 nm), α-amylase (DNS endpoint, A540), α-glucosidase with pNPG (A405), and PTP1B with pNPP (A405). IC_{50} values were obtained by nonlinear regression with appropriate controls and replication.* ***Results:*** *P. emodi contained high flavonoids (852.67 ± 64.97 µg/mL) and tannins (394.00 ± 13.02 µg/mL), with lower phenolics (98.59 ± 29.71 µg/mL). Flavonoids displayed the strongest antiglycation effect (IC_{50} 14.61 ± 0.93 µg/mL), while the n-hexane fraction was the most potent antiglycation extract (9.52 ± 0.34 µg/mL). For α-amylase, phenolics were most active (8.28 ± 1.07 µg/mL) and n-hexane and ethyl acetate fractions were superior (5.99 ± 0.20 and 6.09 ± 1.16 µg/mL), exceeding acarbose (20.54 ± 1.07 µg/mL). Tannins most strongly inhibited PTP1B (4.27 ± 0.20 µg/mL), and the methanol fraction was the most active extract (4.29 ± 0.26 µg/mL), followed by n-hexane (6.73 ± 0.05 µg/mL). For α-glucosidase, phenolics led among classes (5.50 ± 0.56 µg/mL), while n-hexane and methanol fractions were most potent (4.85 ± 0.06 and 5.85 ± 0.69 µg/mL).* ***Conclusion:*** *Paeonia emodi demonstrates a coherent multitarget antidiabetic profile. Non-polar fractions concentrate inhibitors of postprandial pathways (α-amylase/α-glucosidase and antiglycation), whereas polar fractions are enriched for PTP1B inhibition. These complementary mechanisms justify bioassay-guided isolation and standardization efforts toward phytopharmaceutical development for diabetes management.*

Keywords
Paeonia emodi; antiglycation; alpha-amylase; alpha-glucosidase; PTP1B; polyphenols; IC50; diabetes mellitus

INTRODUCTION

Diabetes mellitus is a chronic metabolic disorder characterized by persistent hyperglycaemia resulting from impaired insulin secretion, diminished insulin action, or both (1). Its prevalence continues to rise worldwide, with the fastest growth in low- and middle-income countries and a substantial proportion of cases remaining undiagnosed (2,3). Beyond the direct glycaemic abnormality, diabetes clusters with central adiposity, dyslipidaemia, and hypertension, driving markedly increased risks of microvascular and macrovascular complications and imposing a large societal and economic burden (4,5).

Type 2 diabetes mellitus (T2DM) accounts for the vast majority of cases and is defined pathophysiologically by insulin resistance with progressive β-cell dysfunction (6). At the molecular level, impaired insulin receptor (IR) signalling is central; protein tyrosine phosphatase 1B (PTP1B), a widely expressed non-receptor phosphatase, negatively regulates this pathway by dephosphorylating activated IR and downstream substrates (7). Genetic and pharmacological studies demonstrate that attenuation of PTP1B activity enhances insulin signalling, improves glucose homeostasis, and therefore represents a validated therapeutic strategy for metabolic disease (8,9).

Postprandial hyperglycaemia is a major determinant of overall glycaemic exposure in T2DM and contributes independently to vascular risk (10). Inhibiting intestinal carbohydrate-hydrolysing enzymes—α-amylase, which initiates starch depolymerisation, and α-glucosidase, which catalyses terminal oligosaccharide hydrolysis—slows glucose liberation and absorption, flattening postprandial excursions (11). Approved α-glucosidase inhibitors have established clinical proof-of-concept, yet gastrointestinal adverse effects limit long-term adherence, motivating the search for alternative modulators with improved tolerability and complementary mechanisms (12,13).

Chronic hyperglycaemia also accelerates the formation of advanced glycation end-products (AGEs), which accumulate in long-lived tissues and signal through the receptor for AGEs (RAGE) to amplify oxidative stress and inflammation (14). The AGE–RAGE axis is implicated in the pathogenesis of retinopathy, nephropathy, neuropathy, and atherosclerosis; accordingly, interventions that curb AGE formation or disrupt downstream signalling are attractive adjuncts to glucose-lowering therapy (15,16).

Medicinal plants remain a rich source of bioactive scaffolds that can modulate multiple pathogenic nodes relevant to diabetes, including digestive enzymes, insulin signalling, and carbonyl stress (17). *Paeonia emodi* Wall. ex Royle (Himalayan peony), endemic to the Himalayan region, is used traditionally for cardiopulmonary and gastrointestinal complaints and contains diverse secondary metabolites—monoterpenes, triterpenes, phenolics, and glycosides—consistent with antioxidant and enzyme-modulatory potential (18,19). Preliminary pharmacognostic and pharmacological reports suggest activities compatible with antidiabetic utility, but rigorous target-directed evaluation remains limited (20).

On this basis, we hypothesised that solvent-fractionated extracts of *P. emodi* could deliver multitarget antidiabetic effects: inhibition of α-amylase and α-glucosidase to attenuate postprandial glucose surges; inhibition of PTP1B to enhance insulin receptor signalling; and suppression of AGE formation to mitigate mechanisms of chronic complication (11,14,18–20). The present study therefore (i) quantified α-amylase and α-glucosidase inhibition, (ii) assessed PTP1B inhibitory activity, and (iii) evaluated anti-glycation effects in model systems across *P. emodi* fractions, providing a coherent pharmacological rationale and lead direction for further isolation and characterisation of active constituents (8,9,17–20).

MATERIAL AND METHODS

Plant material and identification

Roots of *Paeonia emodi* Wall. ex Royle were collected in March 2018 from Pir Khana, District Shangla, Khyber Pakhtunkhwa, Pakistan. Botanical identification was performed by Prof. Mehboob-Ur-Rahman. A voucher specimen was deposited in the Herbarium of the Department of Botany, Government Afzal Khan Lala Postgraduate College, Matta, Swat (voucher no. 2017–2019). Additional dried roots (August 2019) were used for extractions. A set of solvent fractions prepared from these roots was provided by Dr. Nida Ambreen (Department of Chemistry, Abdul Wali Khan University, Mardan) for bioassays.

Chemicals and reagents

Analytical-grade solvents and reagents were used: ethanol (95%), n-hexane, chloroform (trichloromethane), ethyl acetate, DMSO, Folin–Ciocalteu reagent, Na_2CO_3, $AlCl_3 \cdot 6H_2O$, $NaNO_2$, NaOH, bovine serum albumin (BSA), D-glucose (anhydrous), p-nitrophenyl-α-D-glucopyranoside (pNPG), p-nitrophenyl phosphate (pNPP), dithiothreitol (DTT), EDTA, phosphate and citrate buffers, and 3,5-dinitrosalicylic acid (DNS). Reference standards: quercetin (flavonoids), gallic acid (phenolics), tannic acid (tannins), acarbose (α-amylase/α-glucosidase), and rutin (antiglycation). Absorbance and fluorescence were read on a calibrated microplate reader.

Preparation of extracts and solvent fractions

Cleaned, shade-dried roots were cut and milled to a coarse powder. Powder was macerated in 95% ethanol (1:10, w/v) in airtight containers for 14–15 days at room temperature with occasional stirring. Filtrates were combined and concentrated under reduced pressure at 45–50 °C to obtain the crude ethanolic extract. The concentrate was suspended in distilled water and successively partitioned with n-hexane, chloroform, and ethyl acetate (three extractions each; ≈1:1 v/v per wash) in a separatory funnel. Organic layers were evaporated to dryness to yield n-hexane, chloroform, and ethyl acetate fractions; the remaining aqueous phase was retained where specified. Dried fractions were stored in amber vials at 4 °C.

Total flavonoid content (TFC)

Following an $AlCl_3$ colorimetric assay, 5 g plant material were extracted in 50 mL 80% ethanol (37 °C, 24 h; centrifuged; supernatant stored at 4 °C). For assay, 500 µL sample were mixed with 1.25 mL water and 75 µL 5% $NaNO_2$; after 5 min, 150 µL 10% $AlCl_3 \cdot 6H_2O$ were added; after 6 min, 500 µL 1 M NaOH and 275 µL water were added. Absorbance was read at **415 nm** against a solvent blank. Quercetin (1000–7.81 µg/mL) provided the calibration curve. Measurements were performed in triplicate.

Total phenolic content (TPC)

TPC was determined by the Folin–Ciocalteu method. Where applicable, samples were defatted (2 g in 50 mL diethyl ether; 15 min, water bath). Reaction mix: 1 mL sample + 1 mL Folin–Ciocalteu reagent; after 3 min, add 1 mL 20% (w/v) Na_2CO_3 and bring to 10 mL with water. Incubate **90 min in the dark** and read at **725 nm**. Gallic acid (1000–7.81 µg/mL) was used for calibration. Triplicates were run.

Total tannin content

Following a standardized Folin-based procedure, 2 g material were extracted in 400 mL 70% acetone (24 h, shaker; 4 °C storage). Tannic acid standards were prepared by serial dilution. For assay, samples/standards were reacted with 500 µL Folin phenol reagent and 2.5 mL Na_2CO_3 solution; absorbance was read at **725 nm**. Triplicate measurements were obtained.

Alkaloid content (acid–base, gravimetric)

Dried sample (5 g) was extracted with 50 mL ethanol (37 °C, 24 h), filtered, and the filtrate acidified with 1% HCl. After holding at 4 °C (~72 h), the solution was basified to pH 8–10 and extracted with chloroform. The organic phase was dried and evaporated; alkaloids were expressed gravimetrically relative to starting mass.

Antiglycation (BSA–glucose) assay

A BSA–glucose model was used in 96-well plates (final **60 µL** per well): 20 µL BSA + 20 µL glucose + 20 µL test fraction or vehicle. Glycated control: 20 µL BSA + 20 µL glucose + 20 µL phosphate buffer. Blank: 20 µL BSA + 40 µL buffer. Plates were sealed and incubated **7 days at 37 °C**. Reactions were stopped with **60 µL cold trichloroacetic acid (TCA)**, followed by centrifugation (15,000 rpm, 4 °C, 4 min). Supernatants were discarded; pellets (AGEs) were dissolved in **60 µL PBS**. Fluorescence was recorded at **Ex 370 nm / Em 440 nm**. Rutin served as the positive control. Percentage inhibition was calculated versus glycated control.

α-Amylase inhibitory assay (DNS endpoint)

An adapted DNS method was run in microplates using a heating step for color development. For each well: 20 µL test fraction (serial dilutions in DMSO; vehicle ≤10% v/v in-well), 50 µL sodium phosphate buffer (**50 mM, pH 6.9**), and 20 µL soluble starch were pre-equilibrated (5 min, 37 °C). The reaction was initiated with 10 µL α-amylase and incubated **20 min at 37 °C**. DNS reagent (100 µL) was added to stop the reaction, plates were transferred to a heating block (**95 °C, 5 min**), cooled on ice, and diluted with 100 µL water. Absorbance was read at **540 nm**. Acarbose was the reference inhibitor. Inhibition (%) was calculated relative to enzyme control without inhibitor.

PTP1B inhibition assay

PTP1B activity was measured using pNPP as substrate in a citrate buffer. Wells received 100 µL PTP1B (0.5 µg/mL in **50 mM citrate, pH 6.0**, containing 0.1 M NaCl, **1 mM DTT**, **1 mM EDTA**) and 2–20 µL test fraction (in DMSO; final DMSO ≤10% v/v), adjusted to volume with buffer, and pre-incubated **10 min at 30 °C**. The reaction was initiated with 100 µL pNPP (final 2 mM) and incubated **30 min at 37 °C**. The reaction was stopped with **10 µL 10 M NaOH**, and absorbance was read at **405 nm**. Inhibition (%) was calculated versus enzyme control.

α-Glucosidase inhibitory assay (pNPG substrate)

Reactions (final **200 µL** per well) contained 130 µL phosphate buffer (**50 mM, pH 6.8**), 10 µL α-glucosidase, and 20 µL test fraction or vehicle (DMSO ≤10% v/v). After **5 min pre-incubation at 37 °C**, 40 µL pNPG (final 2–5 mM) were added and the plate incubated **30 min at 37 °C**. Reactions were stopped with **100 µL 0.2 M Na_2CO_3** to stabilize p-nitrophenolate, and absorbance was read at **405 nm**. Acarbose served as reference. Inhibition (%) was calculated versus enzyme control.

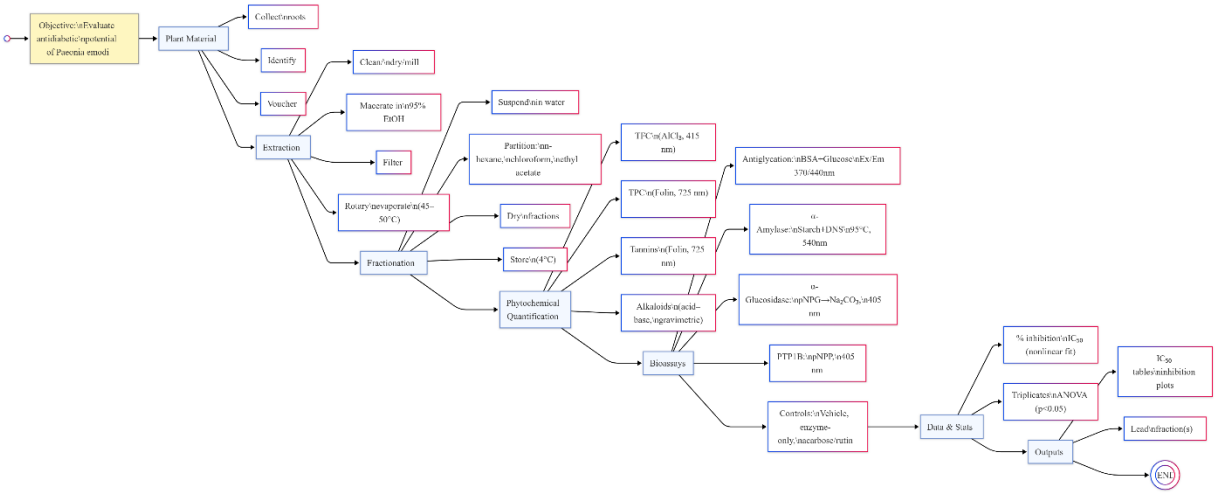

Figure 1 Study Flowchart

Data analysis

All measurements were performed at least in triplicate independent wells per concentration unless otherwise stated. For each assay, percentage inhibition was computed relative to the appropriate control. Concentration–response curves and **IC_{50}** estimates (mean ± SD) were obtained by nonlinear regression (four-parameter logistic) in GraphPad Prism (GraphPad Software). Where multiple fractions were compared, one-way ANOVA with Dunnett's post-hoc test versus control was applied; **$p < 0.05$** was considered statistically significant.

RESULTS

Flavonoids, phenolics, tannins, and alkaloids were quantified spectrophotometrically (TFC at 415 nm; TPC and tannins at 725 nm) or gravimetrically (alkaloids). Standard curves for quercetin and gallic/tannic acid showed excellent linearity across 7.81–1000 µg/mL (Figure 1A–B). *P. emodi* contained the highest levels of flavonoids, followed by tannins, with lower phenolic and alkaloid contents (Table 1). All phytochemical classes inhibited AGE formation in a concentration-dependent manner (Ex/Em 370/440 nm), with flavonoids most potent (IC_{50} = 14.61 ± 0.93 µg/mL). Among solvent fractions, n-hexane showed the strongest antiglycation effect (IC_{50} = 9.52 ± 0.34 µg/mL), outperforming ethyl acetate and chloroform; crude methanol was least active (Table 2; Figure 1C–D).

Table 1. Phytochemical content of P. emodi (mean ± SD)

Analyte	Concentration (µg/mL)
Flavonoids	852.67 ± 64.97
Phenolics	98.59 ± 29.71
Tannins	394.00 ± 13.02
Alkaloids	Gravimetric (see Methods)

Dose–response curves (A_{540}) demonstrated robust inhibition by all classes; phenolics were most active (IC_{50} = 8.28 ± 1.07 µg/mL), closely followed by tannins. Across fractions, n-hexane and ethyl acetate were the most potent (IC_{50} ≈ 6 µg/mL), whereas crude methanol was weak (IC_{50} ≈ 63 µg/mL). Acarbose served as reference (IC_{50} = 20.54 ± 1.07 µg/mL) (Table 2; Figure 1E–F). Tannins gave the lowest IC_{50} (4.27 ± 0.20 µg/mL), with phenolics, flavonoids, and alkaloids showing comparable, slightly higher values. Among fractions, methanol was most active (IC_{50} = 4.29 ± 0.26 µg/mL), followed by n-hexane (IC_{50} = 6.73 ± 0.05 µg/mL), ethyl acetate, and chloroform (Table 2; Figure 1G–H). Phenolics were the most potent class (IC_{50} = 5.50 ± 0.56 µg/mL). Fraction screening highlighted n-hexane (IC_{50} = 4.85 ± 0.06 µg/mL) and methanol (IC_{50} = 5.85 ± 0.69 µg/mL) as top performers, with chloroform and ethyl acetate slightly less active (Table 2; Figure 1I–J).

Table 2. IC_{50} (µg/mL, mean ± SE) across assays by phytochemical class

Assay	Phenol	Tannin	Flavonoid	Alkaloid
Antiglycation	85.56 ± 6.31	18.68 ± 0.11	14.61 ± 0.93	104.20 ± 3.75
α-Amylase	8.28 ± 1.07	9.21 ± 0.79	13.75 ± 0.23	22.57 ± 0.45
PTP1B	6.97 ± 0.23	4.27 ± 0.20	7.68 ± 0.66	7.68 ± 0.66
α-Glucosidase	5.50 ± 0.56	11.52 ± 0.98	22.61 ± 1.20	22.78 ± 3.16

Table 2. IC_{50} (µg/mL, mean ± SE) across assays By phytochemical class by solvent fraction

Assay	n-Hexane	Ethyl acetate (ETOAC)	Chloroform (TCM)	Methanol	Reference
Antiglycation	9.52 ± 0.34	13.13 ± 0.93	17.16 ± 0.62	103.40 ± 4.31	Rutin 31.87 ± 1.60
α-Amylase	5.99 ± 0.20	6.09 ± 1.16	7.73 ± 0.43	63.19 ± 1.69	Acarbose 20.54 ± 1.07
PTP1B	6.73 ± 0.05*	9.19 ± 1.07	9.25 ± 0.49	4.29 ± 0.26	—
α-Glucosidase	4.85 ± 0.06	7.00 ± 0.12	6.75 ± 0.12	5.85 ± 0.69	—

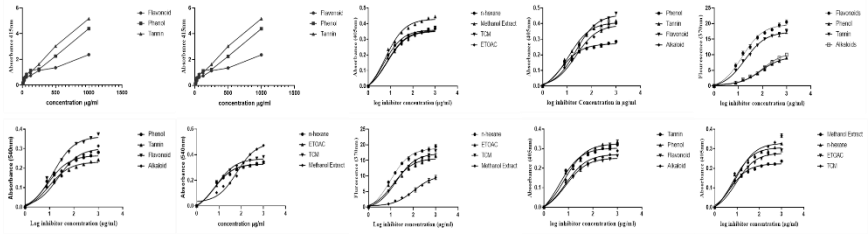

Figure 1. Combined panels. (A–B) Standard curves and content trends for flavonoids/phenolics/tannins. (C–D) Antiglycation dose–response for phytochemical classes and solvent fractions. (E–F) α-Amylase inhibition for classes/fractions. (G–H) PTP1B inhibition for classes/fractions. (I–J) α-Glucosidase inhibition for classes/fractions. Fluorescence is shown for antiglycation; absorbance for enzyme assays.

Figure 2. P. emodi morphology: (A) flower; (B) dried roots used for extraction.

DISCUSSION

This study shows that *Paeonia emodi* possesses multitarget antidiabetic potential spanning digestive-enzyme inhibition, modulation of insulin signalling via PTP1B, and suppression of protein glycation. Phytochemical profiling indicated a predominance of flavonoids with substantial tannin content; phenolics were present at lower levels and alkaloids were minor. These compositional trends were mirrored in bioactivity readouts but with target-specific differences: flavonoids were the most effective antiglycation agents, phenolics led α-amylase and α-glucosidase inhibition, and tannins most strongly inhibited PTP1B. Fraction screening further suggested a polarity split—non-polar n-hexane enriched inhibitors of α-amylase/α-glucosidase and antiglycation, whereas the polar methanolic fraction concentrated PTP1B inhibitors—consistent with chemically distinct actives partitioning into different solvents (1–3).

The antiglycation findings are notable for two reasons. First, the flavonoid-rich class showed low IC_{50} values versus the BSA–glucose model, aligning with established antioxidant and carbonyl-trapping mechanisms by flavonoids and related polyphenols (4,5). Second, n-hexane outperformed other fractions, implying that lipophilic constituents—such as aglycone flavonoids, simple phenolic esters, or terpenoid derivatives—may contribute meaningfully to AGE suppression in this system. Because the BSA assay reads intrinsic AGE fluorescence at Ex/Em 370/440 nm, these effects likely reflect genuine interference with glycoxidation rather than optical artefact; nonetheless, confirmatory non-fluorescent AGE endpoints (e.g., fructosamine, LC–MS adducts) would strengthen this conclusion (6).

For α-amylase and α-glucosidase, phenolic-enriched samples and the n-hexane/ethyl acetate fractions produced sub-10 µg/mL IC_{50} values, exceeding the potency of the reference inhibitor acarbose under our assay conditions. While this supports the presence of strong, possibly dual-target inhibitors, caution is warranted when benchmarking across laboratories: DNS-based α-amylase assays depend on heating steps and matrix colour, and pNPG-based α-glucosidase assays can vary by enzyme source and buffer composition (7,8). Kinetic evaluation (competitive vs non-competitive), counter-screens against unrelated hydrolases, and interference controls (inner-filter effects at 405/540 nm) should be included in subsequent work to confirm specificity (7–9).

PTP1B inhibition was driven primarily by tannins among the isolated classes and by the methanol fraction among solvent extracts. This pattern suggests that polar polyphenols (e.g., hydrolysable/condensed tannins) are plausible contributors, consistent with literature where galloylated phenolics and oligomeric procyanidins interact with the PTP1B catalytic pocket and adjacent allosteric sites through hydrogen bonding and π–π contacts (10,11). Importantly, PTP1B is a validated negative regulator of insulin receptor signalling; thus, hits in this assay complement the digestive-enzyme and antiglycation activities by acting downstream of absorption to enhance insulin action (12). However, polyphenol tannins can be promiscuous in vitro. Orthogonal assays using recombinant TC-PTP (counter-target), detergent supplementation, and redox-insensitive readouts will help exclude nonspecific phosphatase inhibition (10).

Taken together, these results support a **multicomponent, multitarget** rationale for *P. emodi*: (i) attenuation of post-prandial glycaemic spikes via intestinal enzyme inhibition, (ii) improved insulin signalling via PTP1B modulation, and (iii) mitigation of glyco-oxidative damage via antiglycation. The fraction trends indicate that bioactivity is distributed across polarity windows, arguing for bioassay-guided fractionation rather than single-step purification. Two practical lead paths emerge: (a) develop a standardized **n-hexane/ethyl acetate enriched extract** optimised for dual α-amylase/α-glucosidase and antiglycation effects; and (b) pursue **polar methanol sub-fractions** for PTP1B-focused optimisation. Synergy testing among top fractions or purified constituents may further enhance efficacy while reducing required doses (2,3,10).

This study has limitations. Assays were biochemical and performed in microplates; matrix effects, protein binding, and metabolic stability were not assessed. IC_{50} values reflect the exact enzyme source and buffer; direct clinical translation is therefore premature (7–9). No cytotoxicity, permeability, or off-target safety profiling was conducted. Finally, the phytochemical classes used (phenolics, tannins, flavonoids, alkaloids) remain broad; pinpointing the exact chemotypes responsible for activity will require targeted analytics.

Future work should therefore (i) implement **bioassay-guided isolation** with UPLC–HRMS/MS dereplication to identify active scaffolds; (ii) perform **enzyme-kinetic and mechanism** studies (Lineweaver–Burk/Global fit; target engagement with CETSA/SPR where feasible); (iii) evaluate **cellular models** for insulin signalling (IR/AKT phosphorylation) and post-prandial handling (Caco-2 glucose transport), plus **non-fluorescent AGE endpoints**; (iv) test **ex vivo/in vivo** efficacy in diet-induced or genetic models of T2DM, with pharmacokinetics and basic toxicology; and (v) develop a **standardised extract specification** (marker compounds + activity windows) to ensure batch-to-batch reproducibility (5,10–12).

CONCLUSION

Paeonia emodi demonstrated a coherent, multitarget antidiabetic profile. Flavonoids were abundant and drove potent antiglycation activity; phenolic-enriched samples produced sub-10 µg/mL inhibition of α-amylase and α-glucosidase; and tannins were the strongest modulators of PTP1B. Fraction screening revealed a polarity split: the **n-hexane** fraction concentrated inhibitors of post-prandial pathways (antiglycation and digestive enzymes), whereas the **methanolic** fraction was enriched for **PTP1B** inhibition. Together, these complementary mechanisms support a plausible strategy for both attenuating glucose excursions and enhancing insulin signalling.

While the findings are internally consistent across assays, they remain preclinical and biochemical. Translation will require bioassay-guided isolation to identify active chemotypes, mechanism-of-action and selectivity profiling (including orthogonal phosphatase counterscreens), and confirmation in cellular and in-vivo models with pharmacokinetics and basic toxicology. As practical next steps, two development paths are justified: (i) a standardized **non-polar extract** optimized for dual α-amylase/α-glucosidase and antiglycation effects, and (ii) a **polar sub-fraction** or purified constituents targeting PTP1B. If validated in downstream studies, *P. emodi* could furnish leads or standardized phytopharmaceutical preparations that engage multiple disease nodes relevant to type 2 diabetes management.

REFERENCES

1. Chatterjee S, Khunti K, Davies MJ. Type 2 Diabetes. Lancet. 2017;389(10085):2239–2251.
2. Cho NH, Shaw JE, Karuranga S, Huang Y, da Rocha Fernandes JD, Ohlrogge AW, et al. IDF Diabetes Atlas: Global Estimates Of Diabetes Prevalence For 2017 And Projections For 2045. Diabetes Res Clin Pract. 2018;138:271–281.
3. International Diabetes Federation. IDF Diabetes Atlas. 7th ed. Brussels: International Diabetes Federation; 2015.
4. Sales PMS, Souza PM, Simeoni LA, Magalhães P, Silveira D. Inhibition Of Alpha-Amylase And Alpha-Glucosidase By Plant Extracts And Phytochemicals: A Systematic Review. Planta Med. 2012;78(8):1–12.
5. Ahamad J, Naquvi KJ, Mir SR, Ali M, Shuaib M. Alpha-Glucosidase Inhibitors From Medicinal Plants: A Review. Pharmacogn J. 2011;3(22):65–73.
6. Tamrakar AK, Maurya CK, Rai AK. PTP1B Inhibitors For Type 2 Diabetes Treatment: A Patent Review 2011–2014. Expert Opin Ther Pat. 2014;24(10):1101–1115.
7. Bakke J, Haj FG. Protein-Tyrosine Phosphatase 1B Substrates And Metabolic Regulation. Trends Endocrinol Metab. 2015;26(6):305–314.
8. Haj FG, Zabolotny JM, Kim YB, Kim HJ, Shulman GI, Kahn BB, et al. Regulation Of Insulin Receptor Signaling By Protein-Tyrosine Phosphatase 1B. J Biol Chem. 2005;280(2):1022–1029.
9. Liu S, Ishikawa Y, Okazaki Y, Yoshida M, Yamashita T, Yokoi N, et al. Protein Tyrosine Phosphatase 1B Negatively Regulates EphA5-Mediated Insulin Secretion In Pancreatic Islets. J Biol Chem. 2014;289(32):22070–22082.
10. Skyler JS, Bakris GL, Bonifacio E, Darsow T, Eckel RH, Groop L, et al. Differentiation Of Diabetes By Pathophysiology, Natural History, And Prognosis. Diabetes. 2017;66(2):241–255.
11. Xiao JB, Högger P. Dietary Polyphenols And Prevention And Management Of Type 2 Diabetes. Nutrients. 2015;7(8):5489–5506.
12. Barros L, Baptista P, Ferreira ICFR. Effectiveness Of AlCl3 And Folin–Ciocalteu Methods For Quantifying Flavonoids And Phenolics In Plant Extracts. Food Chem. 2008;110(4):1040–1045.
13. Akindahunsi AA, Oyetayo FL. Nutritional And Antioxidant Properties Of Tannins In Selected Tropical Plant Foods. Afr J Biotechnol. 2006;5(5):373–379.
14. Edeoga HO, Okwu DE, Mbaebie BO. Phytochemical Constituents Of Some Nigerian Medicinal Plants. Afr J Biotechnol. 2005;4(7):685–688.
15. Ayatollahi AM, Ghiaci M, Dabbagh H, Mollazadeh S. A Microplate-Based BSA–Glucose Assay For Antiglycation Screening. J Pharmacol Toxicol Methods. 2010;61(2):181–186.
16. Xiao J. A Microplate DNS Method For Alpha-Amylase Inhibition Assay With Improved Throughput. Carbohydr Res. 2015;413:12–15.
17. Rouzbehan S, Moeini R, Ghasemi A. Microplate Assay For Alpha-Glucosidase Inhibition Using p-Nitrophenyl-α-D-Glucopyranoside. J Appl Biol Sci. 2017;11(3):1–6.
18. Cui L, Naik MU, Naik UP, Friesel R. A Simple Microplate Assay For Protein Tyrosine Phosphatase 1B Using p-Nitrophenyl Phosphate. Anal Biochem. 2006;353(2):181–186.
19. Ghayur MN, Gilani AH, Rasheed H, Khan A, Iqbal Z, Ismail M, et al. Cardiovascular And Airway Relaxant Activities Of Peony Root Extract. Can J Physiol Pharmacol. 2008;86(11):793–803.

20. Zargar BA, Rather AA, Bhat ZA, Dar MY. Paeonia Emodi Royle: Ethnomedicinal Uses, Phytochemistry, And Pharmacology. Phytochem Lett. 2013;6(2):261–266.
21. Miller GL. Use Of Dinitrosalicylic Acid Reagent For Determination Of Reducing Sugar. Anal Chem. 1959;31(3):426–428.
22. Bernfeld P. Amylases Alpha And Beta. Methods Enzymol. 1955;1:149–158.
23. Kumar S, Narwal S, Kumar V, Prakash O. Alpha-Glucosidase Inhibitors From Plants: Chemistry And Mechanism. Pharmacogn Rev. 2011;5(9):19–29.
24. International Diabetes Federation. IDF Diabetes Atlas Website. Available from: https://diabetesatlas.org. Accessed 2025 Sep 28.